Water Vapor Tracers as Diagnostics for the Regional Hydrologic Cycle

ABSTRACT

Numerous studies suggest that local feedback of evaporation on precipitation, or recycling, is a significant source of water for precipitation. Quantitative results on the exact amount of recycling have been difficult to obtain in view of the inherent limitations of diagnostic recycling calculations. The current study describes a calculation of the amount of local and remote sources of water for precipitation, based on the implementation of passive constituent tracers of water vapor (termed water vapor tracers, WVT) in a general circulation model. In this case, the major limitation on the accuracy of the recycling estimates is the veracity of the numerically simulated hydrological cycle, though we note that this approach can also be implemented within the context of a data assimilation system. In this approach, each WVT is associated with an evaporative source region, and tracks the water until it precipitates from the atmosphere. By assuming that the regional water is well mixed with water from other sources, the physical processes that act on the WVT are determined in proportion to those that act on the model's prognostic water vapor. In this way, the local and remote sources of water for precipitation can be computed within the model simulation, and can be validated against the model's prognostic water vapor. Furthermore, estimates of precipitation recycling can be compared with bulk diagnostic approaches.

As a demonstration of the method, the regional hydrologic cycles for North America and India are evaluated for six summers (June, July and August) of model simulation. More than 50% of the precipitation in the Midwestern United States came from continental regional tracers, and the local source was the largest of the regional tracers (14%). The Gulf of Mexico and Atlantic

4/6/01

Water Vapor Tracers as Diagnostics of the Regional Hydrologic Cycle

Michael G. Bosilovich *
and
Siegfried D. Schubert

Data Assimilation Office
NASA Goddard Space Flight Center Code 910.3
Greenbelt MD

Submitted To J. Hydrometeorology

* *Corresponding author address*: Data Assimilation Office, NASA Goddard Space Flight Center Code 910.3, Greenbelt, MD 20771, mikeb@dao.gsfc.nasa.gov

regions contributed 18% of the water for Midwestern precipitation, but further analysis suggests that the greater region of the Tropical Atlantic Ocean may also contribute significantly. In general, most North American land regions showed a positive correlation between evaporation and recycling ratio (except the Southeast United States) and negative correlations of recycling ratio with precipitation and moisture transport (except the Southwestern United States). The Midwestern local source is positively correlated with local evaporation, but it is not correlated with water vapor transport. This is contrary to bulk diagnostic estimates of precipitation recycling. In India, the local source of precipitation is a small percentage of the precipitation owing to the dominance of the atmospheric transport of oceanic water. The southern Indian Ocean provides a key source of water for both the Indian continent and the Sahelian region.

1. Introduction

Interannual variability of hydrometeorology (e.g. drought and flood) can have a devastating impact on a region's society and economy. Improved understanding of the variability and extremes of the hydroclimate through diagnostic study should benefit long-term forecasting, disaster preparedness and allocation of resources (e.g. energy and water conservation). In the present study, we have implemented water vapor tracers (WVT) in a general circulation model (GCM) to evaluate their usefulness as a diagnostic of the atmospheric hydrologic cycle. The WVTs are able to distinguish between different regional sources of water that contribute to precipitation. The purpose of the present paper is to present the formulation and validation of the WVTs, and discuss the added information they provide to a GCM simulation.

Koster et al. (1986) introduced passive tracers in a GCM that have a source equal to the evaporation from a prescribed continent or ocean, and used model sources and sinks of water (condensation, reevaporation, convection and advection) to compute tendencies of the passive tracer. In this way, water was "tagged" and followed until it precipitated from the atmosphere. Their results differentiated between continental and oceanic sources of water vapor that contribute to precipitation. The simulations were performed with coarse resolution (8° × 10°, 9 layers) and results for one month periods. The amount of water that evaporates and then precipitates within the same region (precipitation recycling, as defined by Eltahir and Bras, 1996) was not addressed.

Joussaume et al. (1986) describe a similar method of diagnosing the origin of precipitation as "macro-Lagrangian", because water from a distinct region is predicted as a passive constituent of the atmosphere. The formulation of sources and sinks of water vapor tracers is discussed in detail, including evaporation, condensation, re-evaporation, diffusion, advection and convection. The water vapor tracer is predicted forward in time from its source by surface evapotranspiration until it precipitates back to the surface, including all the model-simulated processes that act on the model's prognostic water vapor. That effort demonstrated the range of influence of the oceans on continental precipitation, but did not evaluate local precipitation recycling or the interannual variability of the source regions. Nonetheless, these experiments described a methodology that should also provide significant diagnostic information when studying regional hydrologic cycles (such as those associated with the North American and Indian monsoons). Recently, Numagati (1999) used this methodology to study the Eurasian regional sources of precipitation.

In order to diagnose the sources of North American precipitation, Dirmeyer and Brubaker (1999) used a diagnostic method of analyzing quasi-isentropic back-trajectories of water vapor. The method uses six-hourly estimates of NCEP reanalysis wind, water vapor and evaporation and hourly precipitation observations to determine the regional sources of precipitation. An advantage to this method is that the sources of data are quite flexible. Another advantage is that the computations are less intensive than performing multi-year GCM simulations or reanalyses. However, the initialization of the quasi-isentropic tracers depends on a statistical distribution of the precipitation, and the movement and extraction of water does not depend on the physical tendencies included in the reanalysis. The back-trajectory method does provide estimates of precipitation recycling.

Brubaker et al. (1993) and Eltahir and Bras (1994) describe bulk diagnostic methods that evaluate monthly mean precipitation, evaporation and moisture transport to compute precipitation recycling (quantitatively defined as the recycling ratio). Further studies by Trenberth (1999) and Bosilovich and Schubert (2001) used these models to evaluate the spatial and interannual variability of the local source of water (precipitation recycling). While these methods are computationally efficient, they may be hindered by simplifications, most notably, a lack of short time scale correlations between the hydrological parameters (in particular the diurnal and synoptic time scales). These models provide solely the local source of water and do not include the remote sources of water for a region.

This paper describes the implementation and validation of regional water vapor tracers in a GCM in order to test the tracers in a GCM study of the regional hydrologic cycle. Section 2 describes the model structure, experimental design, and tracer formulation. In section 3, the model water, precipitation, and the WVTs are validated, and the local and remote sources of water for precipitation over India and North America are examined. The precipitation recycling from the WVTs is compared to bulk diagnostic recycling methods.

2. Model and Methodology

a. GEOS GCM

The base model used in this study is version 3 of the Goddard Earth Observing System (GEOS-3) GCM (Suarez and Takacs 1995). The advection is calculated by a positive definite semi-Lagrangian method (Lin and Rood, 1996) on the Arakawa C grid. The model physics includes: Relaxed Arakawa-Schubert (RAS) convection (Moorthi and Suarez, 1992) with reevaporation of falling rain (Sud and Molod 1988), parameterization of shortwave radiation (Harshvardhan et al. 1987) and longwave radiation (Chou 1984), and a level 2.5 boundary layer turbulence closure scheme (Helfand and Labraga, 1988). Recent improvements to the GEOS GCM include the addition of the Mosaic land-surface model (Koster and Suarez, 1992), and the incorporation of sub-grid moist processes in turbulent diffusion (Helfand et al. 1999). The Mosaic land-surface model includes prognostic soil water, temperature and snow, as well as mosaic heterogeneity. The GEOS-3 GCM is a component of the GEOS-3 data assimilation system that is being used to support the EOS Terra and Aqua missions at NASA.

b. Water Vapor Tracers (WVTs)

The implementation of water vapor tracers (WVTs) utilizes existing GEOS-3 code for generic passive constituent tracers including transport and boundary layer turbulent transport processes. In addition, we compute the tendencies of tracer water due to precipitation processes proportional to the prognostic water vapor variable. We emphasize that, while the prognostic water vapor is of course interactive, the WVTs are entirely passive. The prognostic equation for water vapor is,

$$\frac{\partial q}{\partial t} = -\nabla_3 \cdot (qV) + \frac{\partial q}{\partial t}_{turb} + \frac{\partial q}{\partial t}_{cond} + \frac{\partial q}{\partial t}_{revp} + \frac{\partial q}{\partial t}_{RAS} \tag{1}$$

The transport of water is critical to this experiment. Joussaume et al. (1986) suggest that a positive definite advection scheme is required for tracer transport, and they employed a forward scheme. In the present study, the model calculates advection by a positive definite semi-Lagrangian scheme developed by Lin and Rood (1996). Tests with a fourth order advection scheme demonstrated that significant corrections are needed to compute the WVTs due to filling of negative values. At any one point in the atmosphere, the physical tendencies that act on the water vapor are turbulence (*turb*, equation 1 includes surface evaporation), condensation (*cond*), rain evaporation (*revp*) and redistribution by the Relaxed Arakawka Schubert convection (*RAS*).

The prognostic equation for any one tracer is,

$$\frac{\partial q_T}{\partial t} = -\nabla_3 \cdot (q_T V) + \frac{\partial q_T}{\partial t}_{turb} + E_{surf} + f_C \frac{\partial q}{\partial t}_{cond} + f_R \frac{\partial q}{\partial t}_{revp} + f_{RAS} \frac{\partial q}{\partial t}_{RAS}. \tag{2}$$

Turbulent tendency of the water vapor tracers occurs whenever tracer water is present, but surface evaporation may only be occurring in a tracer's finite source region. Further, evaporative sinks of tracers (dew formation) is considered proportional to the ratio of tracer water and total water vapor. Tracer water is assumed to be well mixed with the total water vapor. Therefore, the physical tendencies of tracer water by precipitation processes are computed proportional to the tendencies of total water vapor. The proportionality relationships for condensation (f_C), reevaporation (f_R) and RAS (f_{RAS}) are given by,

$$f_C(L) = \frac{q_T(L)}{q(L)},$$

$$f_R(L) = \frac{\int_1^{L-1}\left(\frac{\partial q_T}{\partial t}_{cond} + \frac{\partial q_T}{\partial t}_{revp}\right)d\sigma}{\int_1^{L-1}\left(\frac{\partial q}{\partial t}_{cond} + \frac{\partial q}{\partial t}_{revp}\right)d\sigma}, \tag{3}$$

$$f_{RAS}(L) = \begin{cases} \dfrac{q_T(L)}{q(L)} & \dfrac{\partial q}{\partial t}_{RAS} < 0 \\ \dfrac{\int_{LM}^{L+1}\frac{\partial q_T}{\partial t}_{RAS}\, d\sigma}{\int_{LM}^{L+1}\frac{\partial q}{\partial t}_{RAS}\, d\sigma} & \dfrac{\partial q}{\partial t}_{RAS} > 0 \end{cases}$$

(L is a given model level, LM is the lowest model level, integrations are done on the sigma vertical coordinate)

The proportionality rules can be summarized by: sinks of tracer water consider the ratio of tracer water to water vapor at a level (e.g. condensation of water), while the sources of tracer water consider the ratio of vertically integrated stores of tracer water and water vapor during vertical processes at a given time (e.g. reevaporation of falling water). RAS acts to redistribute water from lower levels to upper levels.

It should be reiterated that the WVTs are being computed at the model times step as prognostic equations, but there is no feedback of the WVTs on the modeled processes. The prognostic water vapor variable is used to compute the model precipitation, convection and radiation feedback. The subsequent analysis of the model data will rely on, for the most part, monthly averages. To compute the recycling ratio, we will use monthly total and local precipitation area averaged for each month. This will provide a time series that can be used to determine the seasonal mean and statistical relationships.

c. Experimental design

The above algorithm for the WVTs was implemented in the GEOS-3 GCM. For the experiments described here, the model was run at a horizontal resolution of 2°×2.5°, and 48 vertical levels. Six summer season simulations were performed including tracers for the North American and Indian regions. The seasonal simulations are initialized on May 1 (for years 1990-1995) from an existing 10-year model simulation and run through the end of August. Sea surface temperature and sea ice are prescribed from monthly observations. Thirteen regional tracers are defined. A fourteenth tracer is defined as the complement of the 13 regions (includes surface evaporation from the rest of the globe). Note that because each grid point's evaporation is included in one and only one WVT, the sum of all WVTs should compare to the GCMs prognostic specific humidity. All regional tracers are initialized at zero, while the complement tracer is set equal to water vapor at the initial time. Therefore, the sum of all the regional tracers and the complement equal the models' prognostic water vapor at the initial time. Differences that occur later in the simulation will be used to validate the tracer formulation.

Note that we use only thirteen regional tracers, but nineteen regions are identified in Figure 1 between India and North America. Previous studies showed that the Indian Ocean does not have much influence on North America as a source of water (Joussaume et al. 1986, Druyan and Koster 1989). The regional tracers in this experiment cover smaller areas than previous studies. Since it is unlikely that the two regions tracers would interfere, we include the two geographic regions in a single water vapor tracer. For example, this experiment uses the same tracer to account for the southwestern United States (SW) and the India continental (IN) evaporation. The danger is, of course, that IN evaporation could be misdiagnosed as an SW source in North

America. The purpose here is to test the viability of multiple regions in a single WVT as a way to optimize computing resources.

3. Results

In this section, we present the results of the numerical simulations. First, the mean summer (June, July and August – JJA) total precipitable water (TPW) and precipitation are compared with observations. The WVT methodology is validated against the model simulated water variables (TPW and precipitation). Finally, local and remote sources of water for precipitation in the North American and Indian regions are presented and bulk diagnostic methods of computing precipitation recycling are compared with WVT recycling.

a. Simulation of water vapor and precipitation

Figure 2 compares the modeled precipitation and TPW over North America with observations. Compared to the observed TPW (Darnell et al. 1992), GEOS is wetter in the Gulf of Mexico, but drier in the western United States. This contributes to strong gradients of moisture over Mexico. In general, the simulation produces too much precipitation (compared to Xie and Arkin, 1997 observations), in the central United States, the Gulf of Mexico, continental Mexico and the Atlantic Ocean. A swath of large precipitation extends from the central United States to Newfoundland. In the Indian region (Figure 3), the model simulated TPW seems to be comparable to observations (with the only notable exception being that the deserts are drier). The pattern of precipitation matches closely with the observed, but the areas of strong convection show too much modeled precipitation. At the global scale, the model's TPW and precipitation seem to be in line with the observations (Figure 4). While some differences with the observations are apparent, the simulated fields are generally realistic.

b. *Validation of WVTs*

The model predicts global water vapor as described by equation 1. This is entirely separate from the prediction of the WVTs. By design, each grid point's surface evaporation provides a source for only one WVT (one of the 13 regional tracers or the complement tracer). Therefore, the sum of the regional WVTs and the complement WVT should be equal to the model's prognostic water vapor, and we shall use this to determine the uncertainty of the WVT methodology.

Figure 5 compares the model's simulated TPW and precipitation to the sum of all tracer water and the sum of all tracer precipitation from one simulation that was extended several months beyond JJA. The differences (Diff) are globally averaged every three hours. The standard deviation of the global differences (SD) is also included. Regional tracers are initialized at zero while the Complement tracer equals the specific humidity, so that the sum of the tracers is initialized to the model's total water. In the first few weeks, the tracer water spins up to a value that is slightly smaller than the model's water (by -0.05 cm or ~2%). During the spin-up period, there is an overestimate of precipitation by the tracers. The excessive tracer precipitation reduced the total tracer water to a stable point where the tracer precipitation matches the modeled precipitation. So while there is little bias in the global precipitation, the standard deviation of the difference is ~0.2 mm day^{-1} (~5%). Figure 6 shows the zonal mean difference of JJA (all six years) water vapor and total WVTs. The largest difference is ~-0.25 g kg^{-1} near a relative minimum of zonal precipitation (10S – 20S). In general, the differences are small in the lower troposphere, below the convective cloud base, and larger within the cloud.

The error in the WVTs is larger than truncation error, and likely due to simplifications in the tendencies. The only similar data presented in the refereed literature is by Koster et al. (1986). However, only monthly differences are presented, where their regional tracer precipitation shows some small differences compared to the model's simulated precipitation (near ±1%). The last column of Table 1 shows that we obtain similarly small differences for seasonal means.

c. North American local and remote sources of water

In this section, North American (see Figure 1) JJA hydrology is investigated using the WVTs. This region is influenced by a blend of large-scale forcing of the moisture transport (Bermuda High and Rocky Mountains), the Great Plains Low-level Jet and local convective processes (Helfand and Schubert 1995; Higgins et al. 1997; Bosilovich and Sun 1999a). The source regions defined in Figure 1 were designed to isolate significant contributors to precipitation in the central United States.

Figure 7 shows the total precipitation and each regional WVT precipitation over North America. The smallest contour interval (0.1 mm day^{-1}) provides an estimate of the extent of the influence of each region. Southerly flow that dominates the central United States prevents the MW region from influencing SE, and likewise carries SE and SW water into MW. The NW region influences much of North America due to the mean zonal flow. The AT region affects the United States east of the Mississippi River, and it does produce a lot of precipitation from the Gulf of Mexico and Gulf Stream. The Gulf of Mexico strongly affects the SE and MW regions, and even influences the east coast of Canada. A certain amount of water reaches the central United States from MX, but the BO region is not influential northward beyond MX and the southwestward beyond the ITCZ. It is interesting to note that the model tends to produce a high bias swath of precipitation from the central United States to Newfoundland (as much as 1 mm day^{-1} in Figure 2b), but there is not a clear regional, continental or oceanic source tied to the high bias. The model appears to be either producing too much surface evaporation everywhere or the precipitation mechanisms are leading to the bias. It is beyond the scope of this present study to pursue sensitivity and model development. Rather, this points to a potential use of the WVT methodology to diagnose model deficiencies.

Figure 8 shows the mean JJA moisture transport and evaporation, and helps to explain some of the features in Figure 7. Strong evaporation and the easterly flow across the tropical Atlantic Ocean provide the water for the MW and SE regions. Moderate evaporation that occurs in the east SW region is transported by the southerly flow associated with the Low Level Jet into the MW region. The long fetch of the NW region, moderate evaporation toward eastern NW, and zonal flow carry moisture toward the MW region. The EP region shows strong northerly flow along the NW that prevents a lot of moisture from entering the United States. The vertex of this northerly flow and the southerly flow of the Bermuda High occurs between the BO and MX regions. In the mean sense, little water from BO crosses the vertex and moves into the central United States. Rather, as Figure 7 shows, the BO water is carried by the easterly flow to the ITCZ (but some does precipitate in western Mexico). However, moisture evaporated in east MX is far enough from the vertex to be transported by the southerly flow into the United States. The general pattern of the moisture transport (including the southwestern vertex) is comparable to Peixoto and Oort (1992) (their figure 12.17c). While we can use the moisture transport map to discuss the mean circulation of the atmospheric branch of the hydrologic cycle, WVT diagnostics quantify the sources and sinks of the regional hydrology.

Table 1 shows the percentage of precipitation that occurs in each of the land regions from all the WVTs. The time averages are computed from the area average of monthly mean WVT and total precipitation. Despite being a relatively small region (compared to the Brubaker et al. 1993 central United States region), MW provides the largest source of water to the MW region (14.3%) while the sum of AT, TA and GM is about 18%. Regional continental sources make up more than half of the total water that precipitates in the MW region. This shows that the land is a much more important source of water for the Midwest than is implied from only the local source, but it also implies that the quality of the precipitation in this region is strongly influenced by the land parameterization, especially the formulation of evapotranspiration.

The SE region is dominated by the oceanic sources, especially GM. However, recycling does account for 13% of the precipitation and 34% of the sources are unaccounted for by our regional tracers. Some of the unaccounted water is likely related to the tropical Atlantic Ocean closer to Africa (to be examined later in the analysis). The SW sources are diverse, with contributions from most of the nearby regions, though the magnitude of SW total precipitation and recycled precipitation are quite small (Table 2). The NW region exhibits a large local source of precipitation, much larger than the contribution of water from EP. A long fetch, and evaporation that exceeds precipitation, help to explain the importance of the local water source to the NW region during JJA. The MW and SE regions contribute to the NE precipitation due to their proximity, but GM and AT are also very important components. The MX region has some of the largest total and recycled precipitation of the regions studied (Table 2). The lack of a tropical Pacific Ocean source in the regional tracers limits our ability to analyze the MX sources of water.

Figure 9 shows the mean seasonal variation of the sources of water for the MW, SE, SW and MX regions. In the MW region, the sources from GM and TA show an increase during the summer season. The SE source for MW does not show a systematic variation within JJA, but the interannual variability (as denoted by the standard deviation bars) is larger than that of the MW region. Within the SE region, the sources of water from GM and AT (as well as the local source) increase from June to August. Also, there is more variability in August compared to June and July for SE sources from GM and SE.

The SW region has a recycling ratio comparable to SE and MW, but the total precipitation is much smaller (Table 2). The SW recycling ratio (Figure 9) decreases during the course of the summer, while there is an increase of the oceanic sources (GM, AT and TA in Figure 1). The decrease of SW recycling is related to the seasonal decrease of evaporation (1.30, 0.75, 0.64 mm day^{-1} for June, July and August, respectively) and a strong correlation between recycling and evaporation in SW (Figure 10). The MX region exhibits a decrease of the recycling ratio during the summer, while the influence of the BO region increases. This region is known to be strongly impacted by model deficiencies associated with tropical deficiencies. While the sources should be better described by WVTs incorporated into a reanalysis system, these also can be unreliable. For example, Barlow et al. (1998) find that ECMWF reanalysis shows southerly transport for the Mexican region precipitation, while NCEP reanalysis shows easterly flow.

Figure 10 shows the correlations between the recycling ratio (percentage of precipitation that has a local source) and region averaged precipitation, evaporation and moisture transport. In general, the land regions are characterized by a positive correlation between recycling ratio and evaporation and negative correlation with moisture transport. The positive correlation between recycling ratio and evaporation is particularly strong in SW and MX. When moisture transport is strong, the local influence is reduced (see also Bosilovich and Schubert, 2001). It is interesting to note that the MW region shows little correlation with moisture transport. The SE region shows negative correlation with both moisture transport and evapotranspiration. The relationship between precipitation recycling and evaporation will be examined further below.

In order to better understand the relationships between the different source regions, Table 3 shows correlations between the various regions of the percent of regional precipitation they contribute to the MW and SE regions. These are computed from the monthly mean percentage of regional precipitation. Positive values indicate that certain regions are related to each other, likely through the mean circulation. For example, in the MW region, the source from the Gulf of Mexico is related to the sources of the Atlantic and the Tropical Atlantic. In contrast, an increase in the source from the Gulf of Mexico is associated with a decrease in the source from the Eastern Pacific (as indicated by a negative correlation). This information can be used to help understand the relevance of the regions and where additional regions may be needed. In both the MW and SE regions, the Gulf of Mexico is an important source of water and it is positively correlated to the sources from the Tropical Atlantic and Atlantic regions (the SE correlations tend to be weaker). Since the Atlantic sources are farther away, and hence, smaller in magnitude, it may be convenient for some studies to combine all the regions together. It is also useful to correlate the different source regions to the Complement source, in order to identify other regions with important sources. In these experiments, the Complement source in MW is correlated with the Gulf of Mexico, Topical Atlantic and Atlantic regions (Table 3). This indicates we should consider the rest of the Tropical Atlantic (between the Caribbean and Africa) as a regional tracer to help explain more of the regional sources of water for the central United States (the SE correlations are somewhat weaker).

d. Indian local and remote sources of water

The Indian WVTs were computed using the same model constituent tracer arrays as those used for the North American region. The reason for doing this was to test the use of multiple regions in a single tracer to maximize the computational resources and exploit the global model in a regional study. Figure 11 shows the global map of WVT precipitation from the Indian regional tracers along with the companion North American tracers. In general, there is little overlap between the WVTs from the two regions. The most notable exception is the constituent tracer for the Atlantic (AT) and Northern Continental (NC) regions. Precipitation from AT extends very far to the east across Europe, very close to precipitation from NC. However, there is not much influence of AT on the Indian region (IN). In addition, precipitation from SO extends westward across the tropics into South America. While this likely does not interfere with the EC recycling ratio, it may affect the fraction of precipitation associated with EC in MX (Table 1). The percentage of EC precipitation in MX is 0.51%, slightly greater than WC (0.34%) and SW (0.14%). These contributions are small, and do not adversely influence the analysis discussed in the previous section. Nonetheless, if precision is required, multiple regions contributing to a single constituent tracer should not be implemented. However, the overlap of WVT precipitation does not appear overly influential on the regional analysis, so that such a multiple-region tracer approach may be useful in some experiments. The amount of precipitation that occurs in the Indian continental region (IN) from all the North American regions single tracers (MW, SE, TA, GM, MX, BO, EP) is 0.22%.

The southern Indian Ocean (SO) is one of the most influential WVT regions. Its precipitation is noticeable from 60° S to 60° N, and across the tropics to the coast of South America (Figure 11). Druyan and Koster (1989) found that the Indian Ocean did not contribute to the Sahelian precipitation. However, that study considered a region similar to WO, which is dominated by low-level monsoon westerlies. These results indicate that the SO source, which is characterized by low-level easterlies, could impact the Sahelian precipitation.

Water evaporated from the NC region reaches as far east as the Aleutian Islands. The other Indian regional WVTs are much more local. Figure 12 shows the seasonal contributions of the Indian regional WVTs to IN precipitation. The regional WVTs account for 85% of the Indian continental precipitation. The recycling ratios in IN are generally smaller than those in the North American region, but the magnitude of recycled precipitation is larger (due to the larger total precipitation). As a result of the strong low level monsoon winds and the strong oceanic evaporation, WO and SO account for about two-thirds of the water that precipitates over India. The WO sources decrease throughout the summer, while the SO sources increase. The variability of the SO and WO sources is small compared to the variability of the important oceanic sources in North America.

e. Bulk diagnostic recycling

The bulk diagnostic recycling ratios for MW and SE regions have been computed using the methods of Brubaker et al. (1993) and Eltahir and Bras (1994) (as in Bosilovich and Schubert, 2001). These diagnostic routines use monthly mean precipitation, evaporation and vertically integrated moisture transport to compute precipitation recycling, whereas the WVTs are computed at each model time step using the model's physical tendencies. Trenberth (1999) recommends that the bulk diagnostic data be considered as more of an index of precipitation recycling, rather than a quantitative estimate. The WVT precipitation recycling can be considered as a quantitative estimate within the uncertainty discussed earlier and within the context of the GCM simulation. Therefore, the WVT precipitation recycling can be used to validate the simpler bulk diagnostic estimates of precipitation recycling.

Figure 13 shows the MW and SE recycling ratios for each month of the simulation from each method. In the MW region, the WVT recycling ratio is generally between the larger values of Eltahir and Bras (1994) and the lower values of Brubaker et al. (1993). Savenje (1995), Dirmeyer and Brubaker (1999) and Bosilovich and Schubert (2001) all find that the Brubaker method underestimates the precipitation recycling. While this is apparent for the MW region, in the SE region, the WVT recycling ratio is less than the values of both bulk diagnostic methods. However, the SE region also tends not to conform to the typical North American land region (as in Figure 10). The implication is that water evaporated within the SE region is more likely to leave the region, than suggested by both bulk diagnostic methods. Savenjie (1995) attributes the systematic differences of the Brubaker bulk method to using monthly area-averaged hydrologic data. This seems appropriate for the MW region, but does not hold for the SE region.

Figure 10 shows that the SE region WVT recycling does not correlate with the mean hydrology in the same way as the other regions, in that the WVT recycling is negatively correlated to monthly evaporation. Table 4 shows the correlations of the MW and SE regions monthly mean hydrologic data with the bulk diagnostic recycling estimates in addition to the WVT recycling. Similar to the WVT recycling, the bulk diagnostic estimates of recycling are negatively correlated with the evaporation. In the MW region, recycling ratio calculations show correlations with precipitation, evaporation and moisture transport (Table 4) that are different for each recycling calculation. The Eltahir and Bras (1994) recycling ratio is negatively correlated with moisture transport and has little correlation with evaporation. On the other hand, the WVT recycling is positively correlated with evaporation and has little correlation with moisture transport. Despite the mean differences in the SE region, the different recycling methods produce similar correlations, even the atypical negative correlation with evaporation. However, the differences between the MW and SE correlations imply that monthly representations of the precipitation recycling may be inadequate to determine the relationship between evaporation and recycled precipitation, and further investigation of the influence of shorter timescales on precipitation recycling is required.

4. Summary and discussion

In order to compute the local and remote sources of water for regional precipitation, water vapor tracers have been implemented into the NASA GEOS GCM, following Koster et al. (1986) and Joussaume et al. (1986). Six summer seasons were simulated with regional tracers designed to better explain the local and remote sources of water for the central United States and the Indian continental precipitation. The purpose of this experiment is to demonstrate the methodology, validation and analysis of the water vapor tracer methodology applied to regional hydrologic cycles. Model physics affect the specific values of local and remote precipitation and these will vary from model to model. A more rigorous validation of the WVT methodology (compared to previous studies) indicates that our initial implementation of the tracers emulates the model's time and area averaged precipitation and water vapor with acceptably small differences from GCM calculations (typically within 1% of the model's predicted monthly precipitation). The differences arise from simplifications in the tracer tendency calculations and can be large for local instantaneous values (~5% of instantaneous precipitation).[1]

The main results of the analysis of the tracer diagnostics for this simulation are as follows:

1) More than 50% of the precipitation in the Midwestern United States came from continental regional tracers, and the local source was the largest of the regional tracers (at 14%).
2) 18% of Midwestern precipitation came from the Gulf of Mexico and Atlantic Ocean tracers.
3) Statistical correlations suggest that the a portion of the Complement tracer is related to the Gulf of Mexico and Tropical Atlantic sources, so that extending the regional tracers farther east toward Africa may explain more of the central United States precipitation.
4) In general, most North American land regions showed a positive correlation between evaporation and recycling ratio (except the Southeast United States) and negative correlations of recycling ratio with precipitation and moisture transport (except the

[1] We note that recent refinements in our tracer implementation have further reduced these errors to near round-off levels.

Southwestern United States).

5) The bulk diagnostic recycling methods exhibited different means and correlations than the tracer method of recycling in the central United States. However, the bulk diagnostics methods also demonstrated negative correlations of Southeastern evaporation with recycling ratio.

6) The Southeastern United States recycling relationship with the circulation needs to be investigated on shorter time scales than monthly. This could be accomplished with the WVT methodology.

7) Using one tracer array to simulate more than one regional source of water did not overly influence any of the results. However, it can be distracting, and may not be desirable for all purposes.

8) The Western Indian Ocean provides the largest source of water vapor over continental India. This source is larges in June and decreases through August. The Southern Indian Ocean provides a significant source of water for India, but also for the Sahel.

These diagnostic tracers provide additional quantitative information on the regional hydrologic cycle. Such diagnostics would be useful in sensitivity simulations. For example, testing the sensitivity to soil water initialization leads to different local and remote sources of precipitation for wet and dry cases. Without additional diagnostic data, it is impossible to quantify the difference in local and remote sources of water from the difference in precipitation due to thermodynamic perturbations (Bosilovich and Sun 1999 a and b).

While the complement tracer served its purpose for the validation exercise, it would be much more useful if the Complement was broken up into several continental-scale water vapor tracers. In this way, continental and oceanic sources of water for any region could be determined. In addition, the correlation statistics may be better served through correlation with continental scale tracers. The primary deficiency of the WVT methodology is that if the WVTs are not properly defined at the beginning of experimentation, then the simulation will need to be redone. For example, the Midwestern United States precipitation may be better defined by a more rigorous tracking of the tropical Atlantic evaporative sources, and Mexican regional hydrology requires a more careful consideration of the tropical sources of water. This is not an issue with diagnostic approaches (as in Dirmeyer and Brubaker, 1999). Furthermore, the results from a GCM simulation are also limited by the GCMs ability to simulate the physical processes, climate circulation and variability. However, the data can provide additional quantitative analysis of the regional hydrology of climate variations and extremes, within the context of the global model. Applications within a global data assimilation system will provide better estimates of the local and remote sources of water in real data case studies.

Acknowledgments

Drs. Yogesh Sud, Robert Atlas and Paul Dirmeyer have provided many useful discussions on this research. The development of the code has been was completed with assistance from Greg Walker, Andrea Molod and Larry Takacs. This research was partially funded by the Joint GCIP/PACS Warm Season Precipitation Initiative.

5. References

Barlow, M., S. Nigam and E. H. Berbery, 1998: Evolution of the North American monsoon system. *J. Climate*, **11**, 2238 – 2257.

Bosilovich, M. G., and S. D. Schubert, 2001: Precipitation recycling in the GEOS-1 data assimilation system over the central United States. *J. Hydromet.*, **2**, 26 – 35.

Bosilovich, M. G., and W.-Y. Sun, 1999a: Numerical simulation of the 1993 Midwestern flood: Land-atmosphere interactions. *J. Clim.*, **12,** 1490-1505.

Bosilovich, M. G. and W.-Y. Sun, 1999b: Numerical Simulation of the 1993 Midwestern Flood: Local and Remote Sources of Water. *J. Geophys. Res.*, **D 104**, 19415-19424.

Brubaker, K. L., D. Entekahabi and P. S. Eagleson, 1993: Estimation of precipitation recycling. *J. Clim.*, **6,** 1077-1089.

Chou, M. D., 1984: Broadband water vapor transmission functions for atmospheric IR flux computations. *J. Atmos. Sci.*, **41**, 1775-1778.

Darnell, W. L., W. F. Staylor, S. K. Gupta, N. A. Ritchey and A. C. Wilber, 1992: Seasonal variation of surface radiation budget derived from International Satellite Cloud Climatology Project C1 data. *J. Geophys. Res.*, 97, 15741 – 15760.

Dirmeyer, P. A., 1999: Assessing GCM sensitivity to soil wetness using GSWP data. *J. Meteorol. Soc. Japan*, **77**, 367-385.

Dirmeyer, P. A. and K. L. Brubaker, 1999: Contrasting evaporative moisture sources during the drought of 1988 and the flood of 1993. *J. Geophys. Res.*, **104,** 19383-19398.

Druyan, L. M., and R. D. Koster, 1989: Sources of Sahel precipitation for simulated drought and rainy seasons. *J. Climate*, **2**, 1438 – 1446.

Eltahir, E. A. B., and R. L. Bras, 1994: Precipitation recycling in the Amazon basin. *Q. J. R. Meteorol. Soc.*, **120,** 861-880.

Eltahir, E. A. B., and R. L. Bras, 1996: Precipitation recycling. *Rev. of Geophysics*, **34**, 367 – 378.

Harshvardhan, R. Davies, D. A. Randall, and T. G. Corsetti, 1987: A fast radiation parameterization for atmospheric circulation models. *J. Geophys. Res.*, **92**, 1009-1016.

Helfand, H. M., and J. C. Labraga, 1988: Design of a non-singular level 2.5 second order closure model for prediction of atmospheric turbulence. *J. Atmos. Sci.*, **45**, 113-132.

Helfand, H. M. and S. D. Schubert, 1995: Climatology of the simulated Great Plains LLJ and its contribution to the continental moisture budget of the United States. *J. Clim.*, **8**, 784–806.

Helfand, H. M., A. Molod and M. G. Bosilovich, 1999: Implications of a moist turbulence parameterization for the numerical prediction of the structure and properties of the atmospheric boundary layer. 13th Conference on Numerical Weather Prediction, September 13-17, Denver, CO.

Higgins, R. W., Y. Yao, E. S. Yarosh, J. E. Janowiak and K. C. Mo, 1997: Influence of the Great Plains low-level jet on summertime precipitation and moisture transport over the central United States. *J. Clim.*, **10**, 481 – 507.

Joussaume, S., R. Sadourny and C. Vignal, 1986: Origin of precipitating water in a numerical simulation of July climate. *Ocean-Air Interactions,* **1,** 43 - 56.

Koster, R. D., J. Jouzel, R. Suozzo, G. Russell, W. Broecker, D. Rind, and P. Eagleson, 1986: Global sources of local precipitation as determined by the NASA/GISS GCM. *Geophys. Res. Let.,* **13,** 121-124.

Koster, R. D., and M. J. Suarez, 1992: Modeling the land surface boundary in climate models as a composite of independent vegetation stands. *J. Geophys. Res.,* **97,** 2697 - 2715.

Numagati, A., 1999: Origin and recycling processes of precipitating water over the Eurasian continent: Experiments using and atmospheric general circulation model. *J. Geophys. Res.,* **104,** 1957-1972.

Lin, S.-J., and R. B. Rood, 1996: Multidimensional flux form semi-lagrangian transport schemes. *Mon. Wea. Rev.,* **124,** 2046 – 2070.

Moorthi, S. and M. J. Suarez, 1992: Relaxed Arakawa Schubert: A parameterization of moist convection for general circulation models. *Mon. Wea. Rev.,* **120,** 978-1002.

Peixoto, J. P., and A. H. Oort, 1992: *Physics of Climate.* American Institute of Physics. 520 pp.

Savenije, H. H. G., 1995: New Definitions for moisture recycling and the relation with land use change in the Sahel. *J. Hydrol.,* **167,** 57 – 78.

Suarez, M. J., and L. L. Takacs, 1995: Documentation of the ARIES/GEOS dynamical core: Version 2. NASA Technical memorandum 104606 volume 5, NASA Goddard Space Flight Center, Greenbelt, MD.

Sud, Y. C., and A. Molod, 1988: The roles of dry convetion, cloud-radiation feedback processes and the influence of recent improvements in the parameterization of convection in the GLA AGCM. *Mon. Wea. Rev.,* **116,** 2366 - 2387.

Trenberth, K. E., 1999: Atmospheric moisture recycling: Role of advection and local evaporation. *J. Climate,* **12,** 1368 – 1381.

Xie, P., P. A. Arkin, 1997: Global Precipitation: A 17-Year Monthly Analysis Based on Gauge Observations, Satellite Estimates, and Numerical Model Outputs. *Bull. Amer. Meteor. Soc.,* **78,** 2539–2558.

6. Tables

Table 1 Percentage of total precipitation in regions of the first column occurring from evaporation in the regions of the first row, averaged for JJA. Bold values highlight the local source of precipitation (recycling). The difference of the Sum from 100% is associated with the difference of the tracers and modeled precipitation. Comp is the complement WVT and consists of the rest of the globe not included in regional WVTs.

Destination \ Source	MW	SE	SW	NW	WC	EC	NE	AT	TA	GM	MX	BO	EP	Comp	Sum
Midwest (MW)	**14.3**	12.6	4.7	10.1	4.8	2.0	1.2	4.5	3.3	9.9	4.0	1.6	4.3	23.1	100.3
South East (SE)	1.4	**12.7**	1.8	2.0	1.0	0.8	0.7	11.4	9.2	20.0	3.5	0.9	1.3	34.1	101.0
South West (SW)	1.7	4.5	**11.8**	5.8	1.9	0.7	0.5	4.8	5.5	12.0	11.1	4.9	4.6	31.2	101.2
North West (NW)	3.4	1.8	2.7	**26.9**	9.4	1.6	0.9	2.9	1.3	2.6	1.9	1.3	13.0	30.8	100.4
West Canada(WC)	1.9	0.6	0.4	5.9	**28.7**	4.8	0.9	2.1	0.3	0.6	0.3	0.3	15.6	37.3	99.8
East Canada(EC)	8.4	3.7	1.2	5.7	17.8	**16.5**	2.9	2.5	0.9	2.2	1.0	0.5	6.7	29.6	99.6
North East (NE)	11.8	13.9	2.2	5.6	4.5	3.1	**7.8**	9.6	3.5	9.1	2.3	0.8	3.1	23.0	100.4
Mexico (MX)	0.3	1.3	0.4	0.6	0.3	0.5	0.1	4.3	9.5	12.4	**16.9**	8.4	1.0	43.3	99.3

Table 2 Table of North American continental region's precipitation (P), Evaporation (E), recycled precipitation (P_r), percentage of recycled precipitation, percentage of recycled evaporation and area of the region. Note that percentages do not equal the ratios of annual averages on this table, because the percentages are computed from the average of monthly ratios, not the ratio of annual averages.

	P (mm day^{-1})	E (mm day^{-1})	P_r (mm day^{-1})	% of P	% of E	Area (Km^2)
MW	4.31	4.03	0.61	14.26	15.12	1.38E+06
SE	3.37	4.03	0.39	12.72	9.76	1.66E+06
SW	0.59	0.90	0.08	11.81	7.55	1.60E+06
NW	1.77	2.39	0.47	26.89	19.48	2.29E+06
WC	2.62	2.63	0.75	28.71	28.47	3.69E+06
EC	2.53	1.69	0.41	16.50	24.29	3.02E+06
NE	3.68	3.81	0.28	7.83	7.50	9.20E+05
MX	4.66	3.10	0.77	16.94	24.90	1.40E+06

Table 3 Correlation coefficients of all the percentages of source water for the MW region and the SE region (computed from 18 monthly mean values). Positive correlations greater than 0.5 are bold and negative correlations less than –0.5 are bold italic. Rows and columns are sorted by the mean percentage of precipitation from each region so that the largest sources are down to the right.

MW Reg.	*NE*	*BO*	*EC*	*TA*	*MX*	*EP*	*AT*	*SW*	*WC*	*GM*	*NW*	*SE*	*MW*
NE	1.00												
BO	0.16	1.00											
EC	0.48	0.03	1.00										
TA	-0.15	***-0.50***	-0.31	1.00									
MX	-0.10	0.35	-0.11	-0.24	1.00								
EP	**0.51**	0.11	0.24	***-0.65***	0.14	1.00							
AT	0.01	-0.15	-0.34	**0.52**	-0.33	-0.49	1.00						
SW	-0.19	0.10	-0.07	***-0.50***	**0.67**	0.36	-0.32	1.00					
WC	0.30	-0.14	0.44	***-0.55***	-0.20	**0.67**	-0.40	0.26	1.00				
GM	-0.25	-0.42	-0.23	**0.84**	-0.14	***-0.72***	**0.53**	-0.48	***-0.68***	1.00			
NW	-0.22	-0.03	0.19	***-0.55***	0.26	0.39	***-0.74***	0.48	**0.52**	***-0.66***	1.00		
SE	-0.28	0.16	-0.27	-0.34	-0.15	-0.05	0.08	0.01	-0.05	-0.15	-0.06	1.00	
MW	0.21	0.03	0.48	-0.09	***-0.55***	0.03	-0.31	-0.49	0.23	-0.19	0.23	-0.17	1.00
Comp	0.09	0.10	-0.30	**0.65**	-0.12	-0.36	0.37	***-0.51***	***-0.56***	**0.53**	***-0.60***	-0.45	-0.07

SE Reg.	*NE*	*EC*	*BO*	*WC*	*EP*	*MW*	*SW*	*NW*	*MX*	*TA*	*AT*	*SE*	*GM*
NE	1.00												
EC	**0.55**	1.00											
BO	-0.12	0.10	1.00										
WC	0.45	**0.74**	0.30	1.00									
EP	0.09	0.40	**0.64**	**0.76**	1.00								
MW	0.48	**0.67**	-0.11	**0.69**	0.26	1.00							
SW	0.06	0.21	0.40	**0.51**	**0.70**	0.05	1.00						
NW	0.06	0.45	0.39	**0.78**	**0.79**	**0.51**	**0.62**	1.00					
MX	-0.17	0.16	**0.83**	0.40	**0.77**	-0.11	**0.78**	**0.51**	1.00				
TA	-0.42	***-0.56***	-0.04	-0.37	0.08	***-0.64***	0.14	-0.22	0.16	1.00			
AT	0.23	-0.05	***-0.73***	-0.31	***-0.71***	0.01	***-0.66***	***-0.61***	***-0.82***	-0.17	1.00		
SE	**0.59**	**0.57**	-0.40	0.40	-0.14	**0.78**	-0.20	0.19	-0.46	***-0.72***	0.32	1.00	
GM	-0.49	-0.45	-0.14	***-0.56***	-0.44	***-0.56***	-0.28	-0.41	-0.19	0.22	0.13	-0.20	1.00
Comp	-0.39	***-0.52***	0.23	***-0.50***	-0.14	-0.43	-0.20	-0.30	0.08	0.37	-0.18	***-0.66***	-0.20

Table 4 Correlation coefficients (computed from monthly means of six JJAs) of precipitation (P), evaporation (E), moisture transport (QV), Eltahir and Bras (1994) recycling (ρ_E), Brubaker et al. (1993) recycling (ρ_B) and WVT recycling (ρ_T) for MW and SE.

MW	P	E	QV	ρ_E	ρ_B	ρ_T
P	1.00					
E	-0.24	1.00				
QV	0.13	0.49	1.00			
ρ_E	-0.45	0.09	-0.71	1.00		
ρ_B	-0.54	0.44	-0.45	0.86	1.00	
ρ_T	-0.32	0.64	-0.04	0.50	0.75	1.00

SE	P	E	QV	ρ_E	ρ_B	ρ_T
P	1.00					
E	0.24	1.00				
QV	0.64	0.48	1.00			
ρ_E	-0.86	-0.39	-0.78	1.00		
ρ_B	-0.72	-0.23	-0.87	0.86	1.00	
ρ_T	-0.93	-0.35	-0.65	0.90	0.67	1.00

7. List of Figures

Figure 4 (a) Zonal mean JJA TPW (cm) for GEOS (solid) and ISCCP (dashed). (b) Zonal mean JJA precipitation (mm day^{-1}) for GEOS (solid) and Xie and Arkin (1997) (dashed). The averaging period for the observations is the same as Figure 2.

Figure 5 Three hourly time series of globally average mean differences (Diff) and standard deviation (SD) of the global difference map of the model minus WVT for (a) TPW and (b) precipitation. This is one representative year of the six which was continued until mid-December.

Figure 6 Zonal average of the (a) JJA mean specific humidity (solid) and total water vapor tracers (dashed) (b) difference of total water vapor tracers and specific humidity, the solid line indicates cloud top and the dashed line indicates the Relaxed Arakawa Schubert cloud base, and (c) JJA precipitation. The data are time averaged for all six years of JJA. Units are g/kg for specific humidity, water vapor tracer and their difference, and mm day^{-1} for precipitation.

Figure 7 Precipitation (in mm day^{-1}) for the 6 year JJA average of the total, each regional WVT and the complement WVT. The abbreviated name and geographic source region are included in each figure. Bold contour intervals are 0.1, 4, 8 and 16 mm day^{-1} while the light contours are 0.5, 1, 1.5, 2, and 3 mm day^{-1}.

Figure 8 JJA average water vapor transport ([m s^{-1}][g kg^{-1}] vector scale is shown) and evaporation (mm day^{-1}) (contoured with values greater than 4 mm day^{-1} shaded).

Figure 9 Percent contribution of evaporation from the North American regions to precipitation in (a) MW, (b) SE, (c) SW and (d) MX. The bars indicate the monthly means for June, July and August averaged for all six season, and the error bars indicate one standard deviation of the mean.

8. Figures

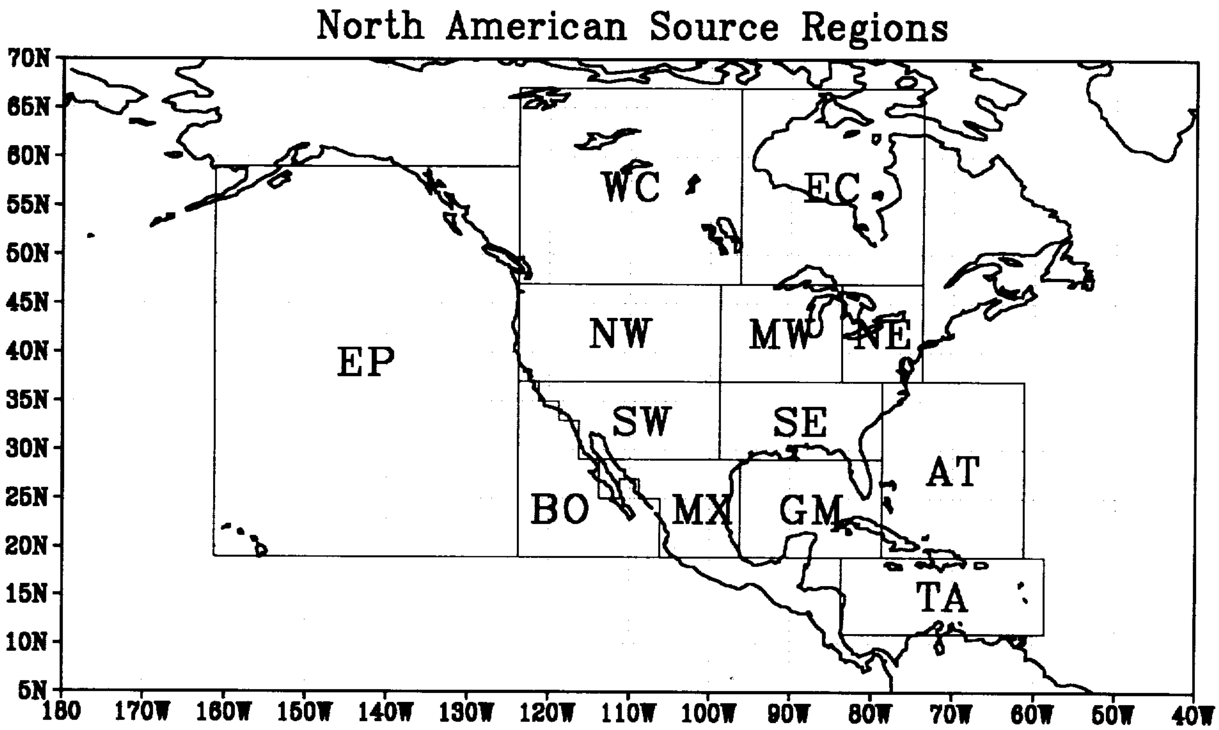

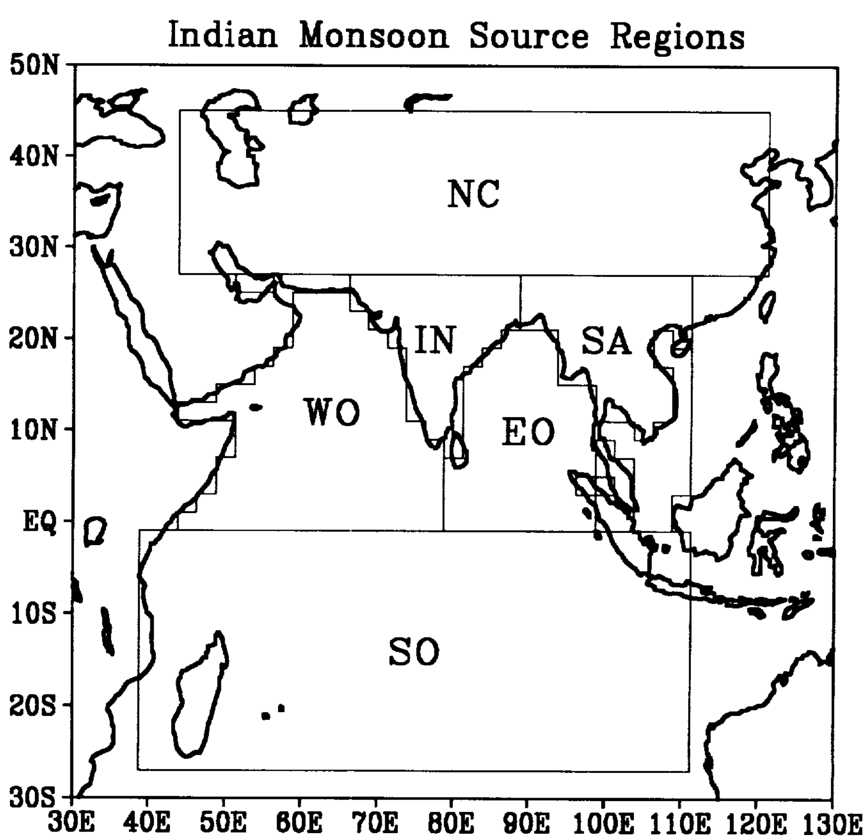

Figure 1

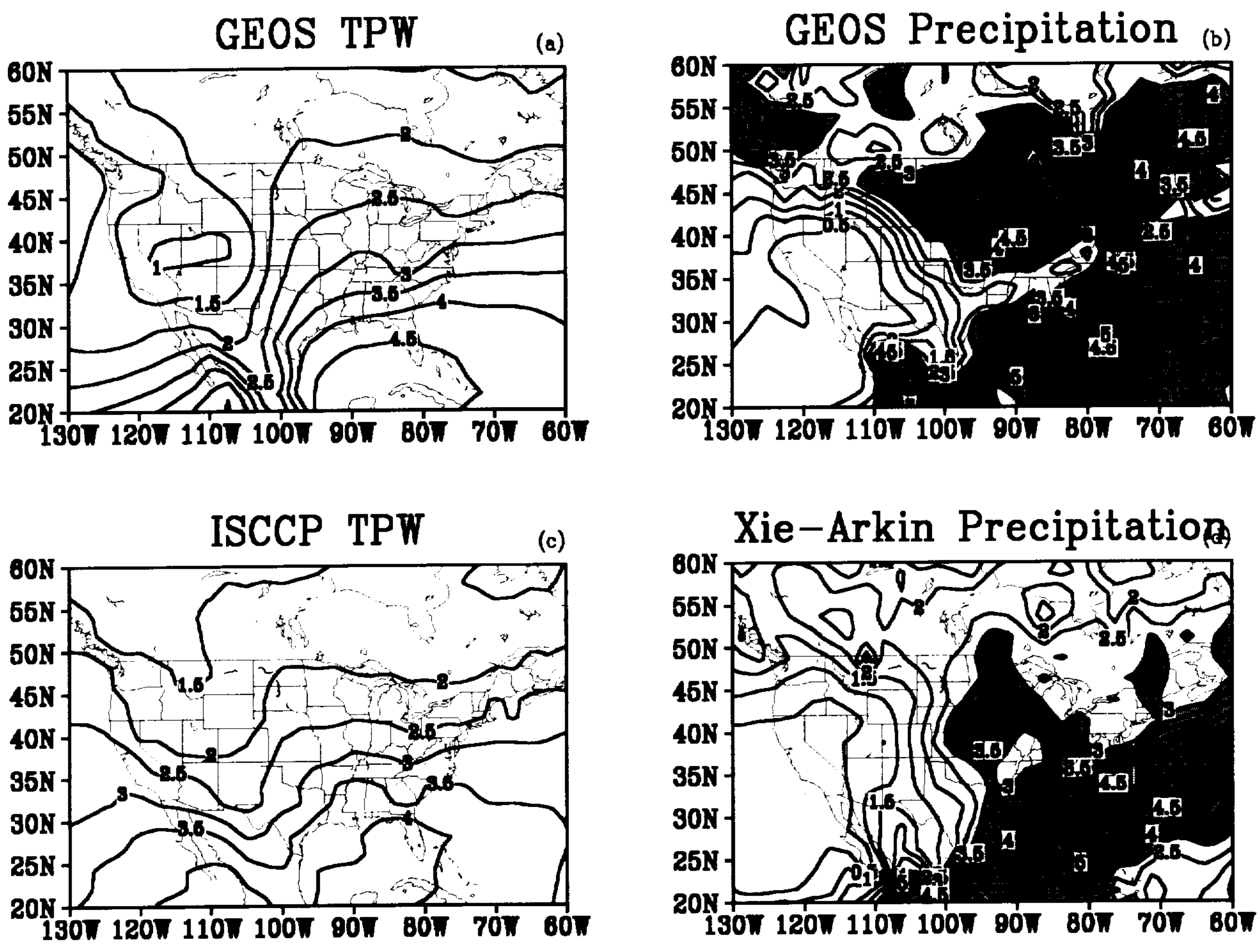
GEOS TPW
(a)
GEOS Precipitation
(b)
ISCCP TPW
(c)
Xie-Arkin Precipitation
(d)
60N
55N
50N
45N
40N
35N
30N
25N
20N
130W 120W 110W 100W 90W 80W 70W 60W

Figure 2

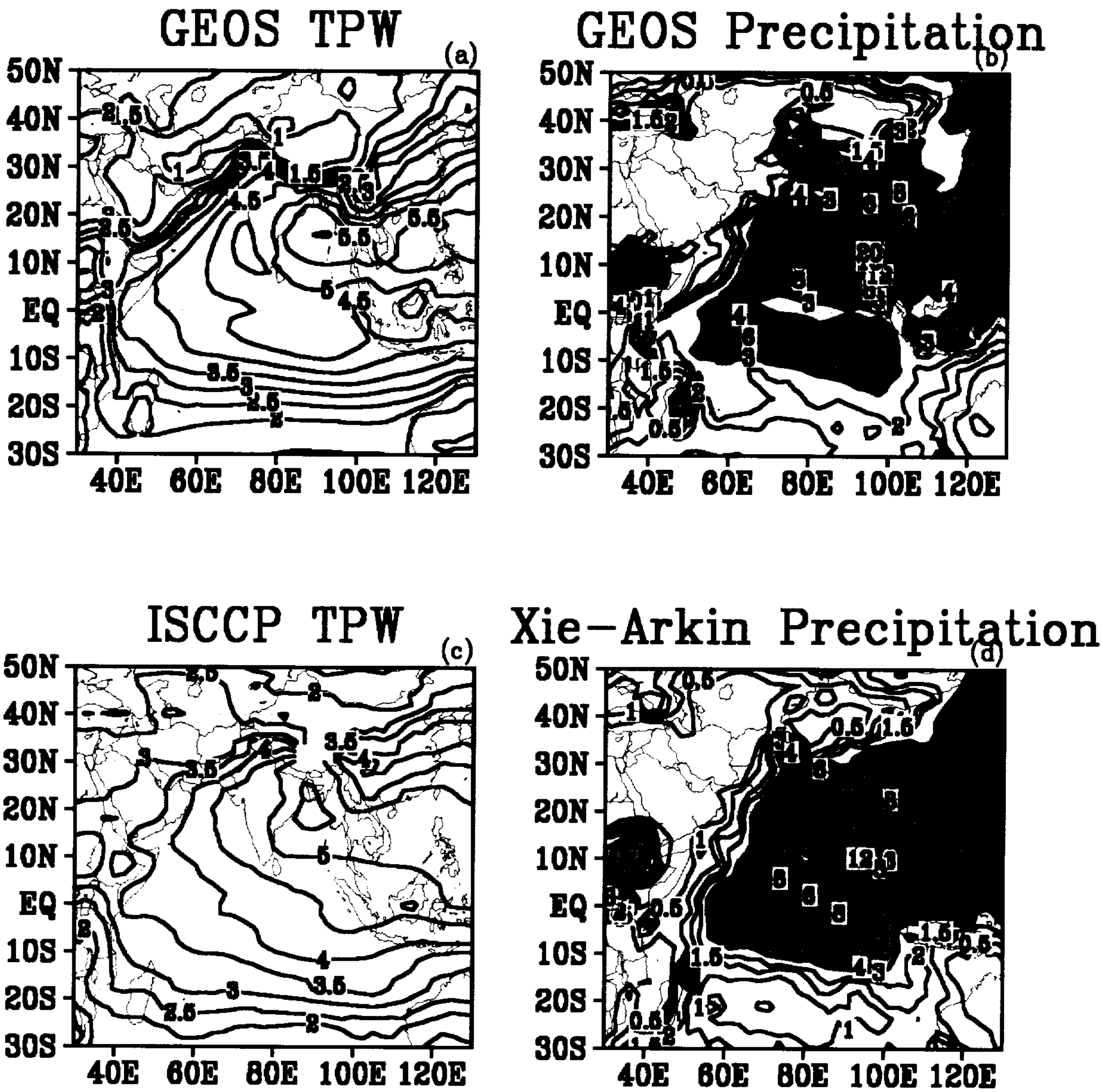
GEOS TPW
(a)
GEOS Precipitation
(b)
ISCCP TPW
(c)
Xie−Arkin Precipitation
(d)
50N
40N
30N
20N
10N
EQ
10S
20S
30S
40E 60E 80E 100E 120E

Figure 3

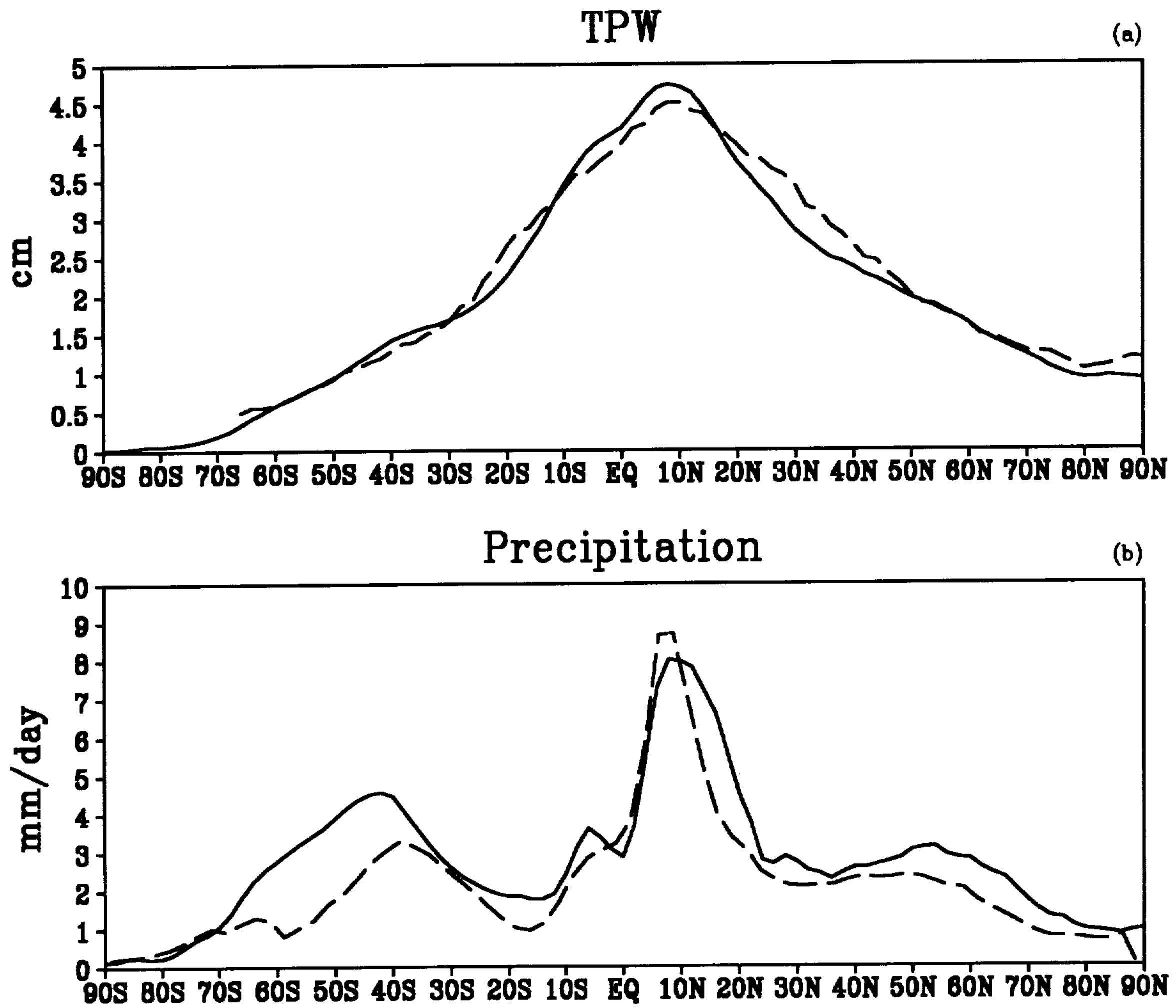
TPW
(a)
cm
5
4.5
4
3.5
3
2.5
2
1.5
1
0.5
0
90S 80S 70S 60S 50S 40S 30S 20S 10S EQ 10N 20N 30N 40N 50N 60N 70N 80N 90N
Precipitation
(b)
mm/day
10
9
8
7
6
5
4
3
2
1
0
90S 80S 70S 60S 50S 40S 30S 20S 10S EQ 10N 20N 30N 40N 50N 60N 70N 80N 90N

Figure 4

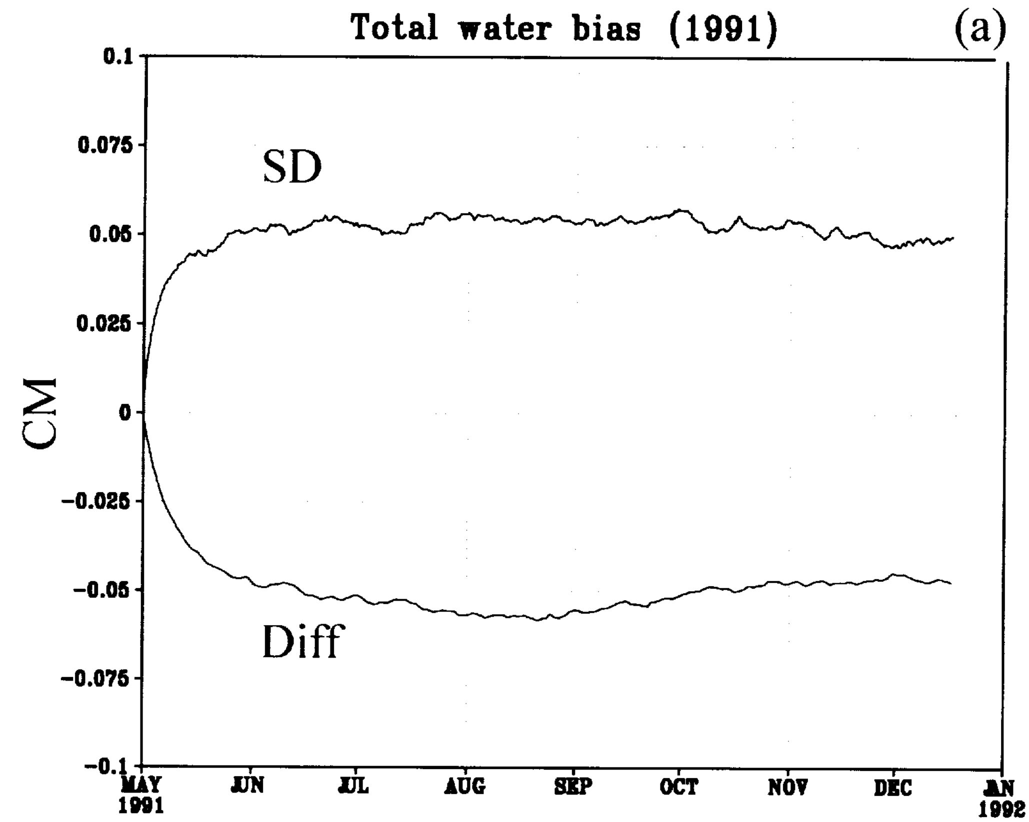

Total water bias (1991)
(a)
CM
SD
Diff
0.1
0.075
0.05
0.025
0
-0.025
-0.05
-0.075
-0.1
MAY 1991
JUN
JUL
AUG
SEP
OCT
NOV
DEC
JAN 1992

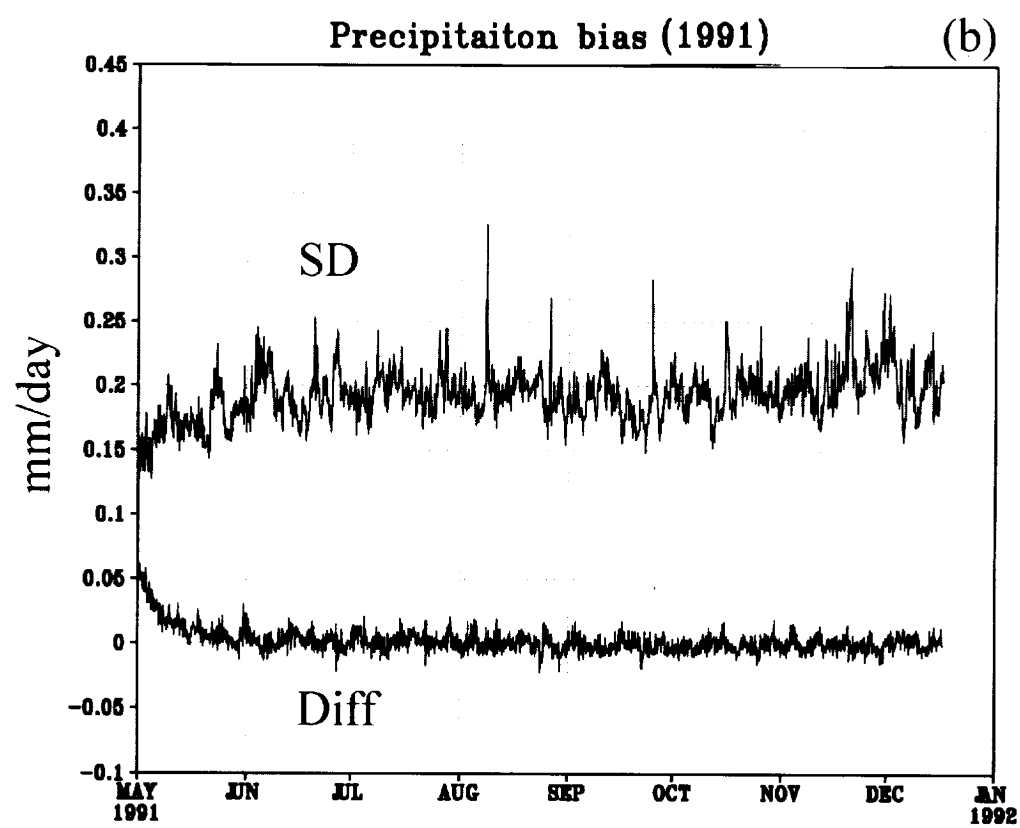

Precipitaiton bias (1991)
(b)
mm/day
SD
Diff
0.45
0.4
0.35
0.3
0.25
0.2
0.15
0.1
0.05
0
-0.05
-0.1
MAY 1991
JUN
JUL
AUG
SEP
OCT
NOV
DEC
JAN 1992

Figure 5

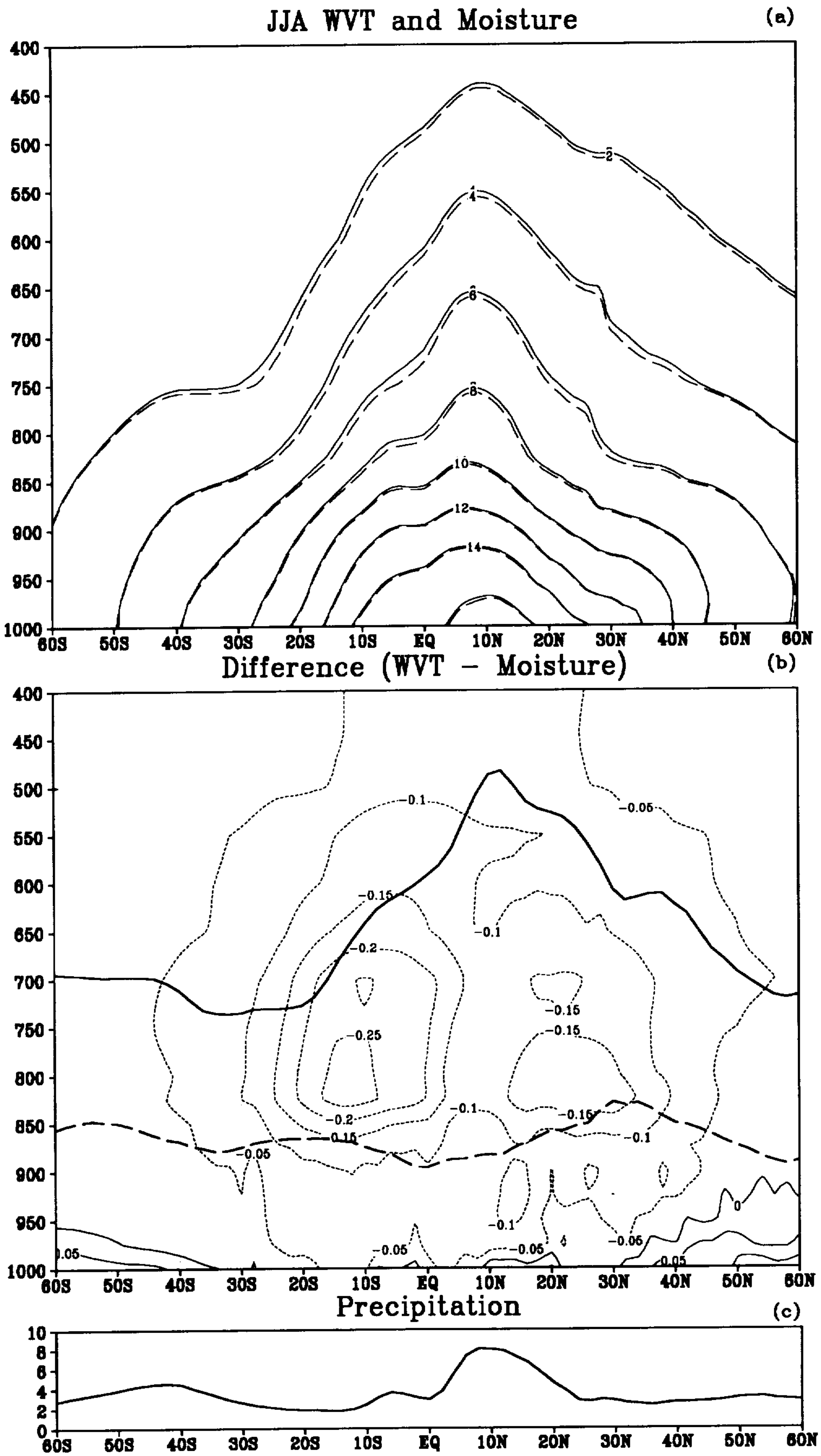

JJA WVT and Moisture
(a)
400
450
500
550
600
650
700
750
800
850
900
950
1000
60S 50S 40S 30S 20S 10S EQ 10N 20N 30N 40N 50N 60N
2
4
6
8
10
12
14
Difference (WVT - Moisture)
(b)
-0.1
-0.05
-0.15
-0.2
-0.25
0
0.05
Precipitation
(c)
10
8
6
4
2
0

Figure 6

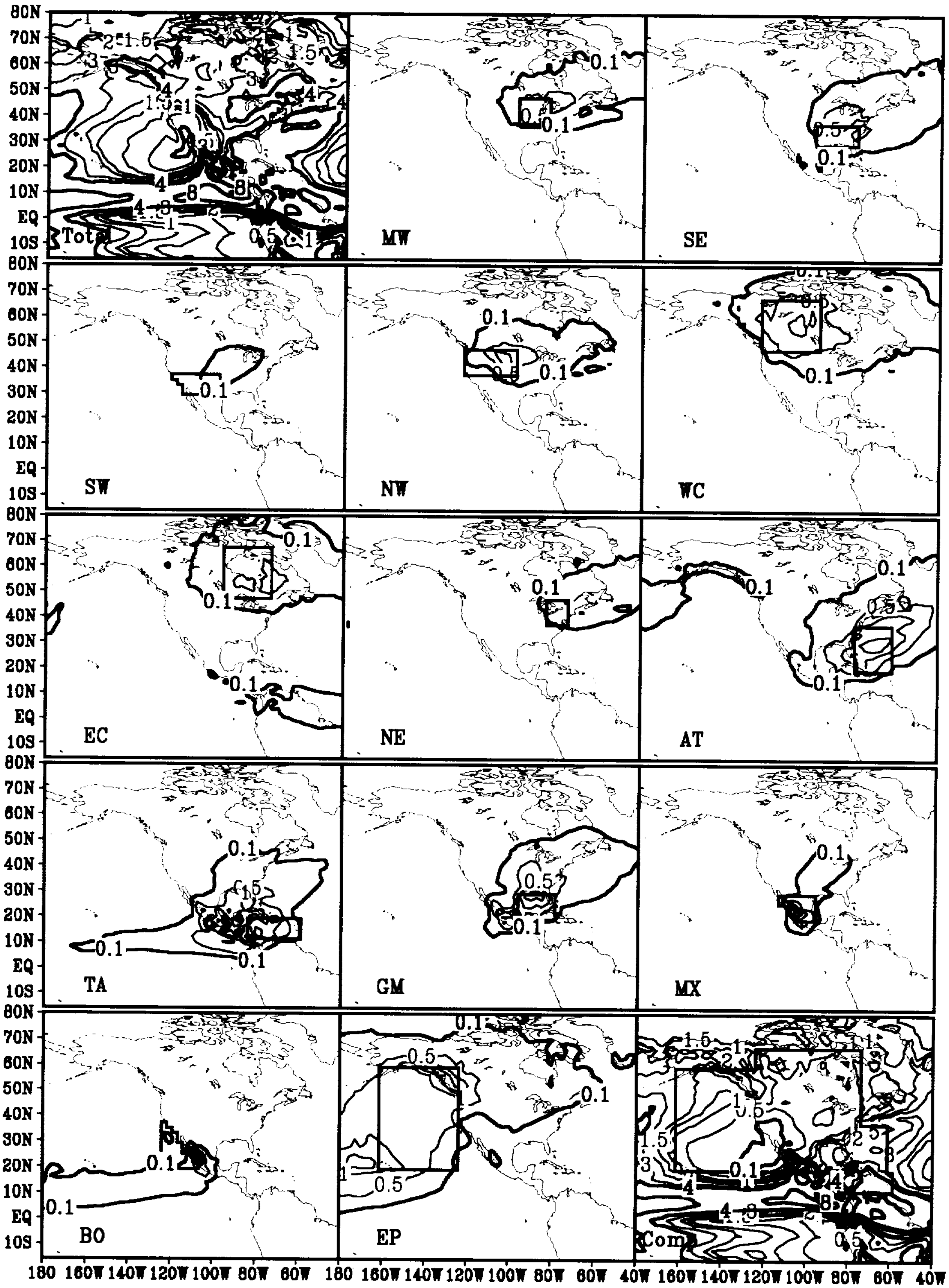
80N
70N
60N
50N
40N
30N
20N
10N
EQ
10S
Total
MW
SE
SW
NW
WC
EC
NE
AT
TA
GM
MX
BO
EP
Com
180 160W 140W 120W 100W 80W 60W
40W

Figure 7

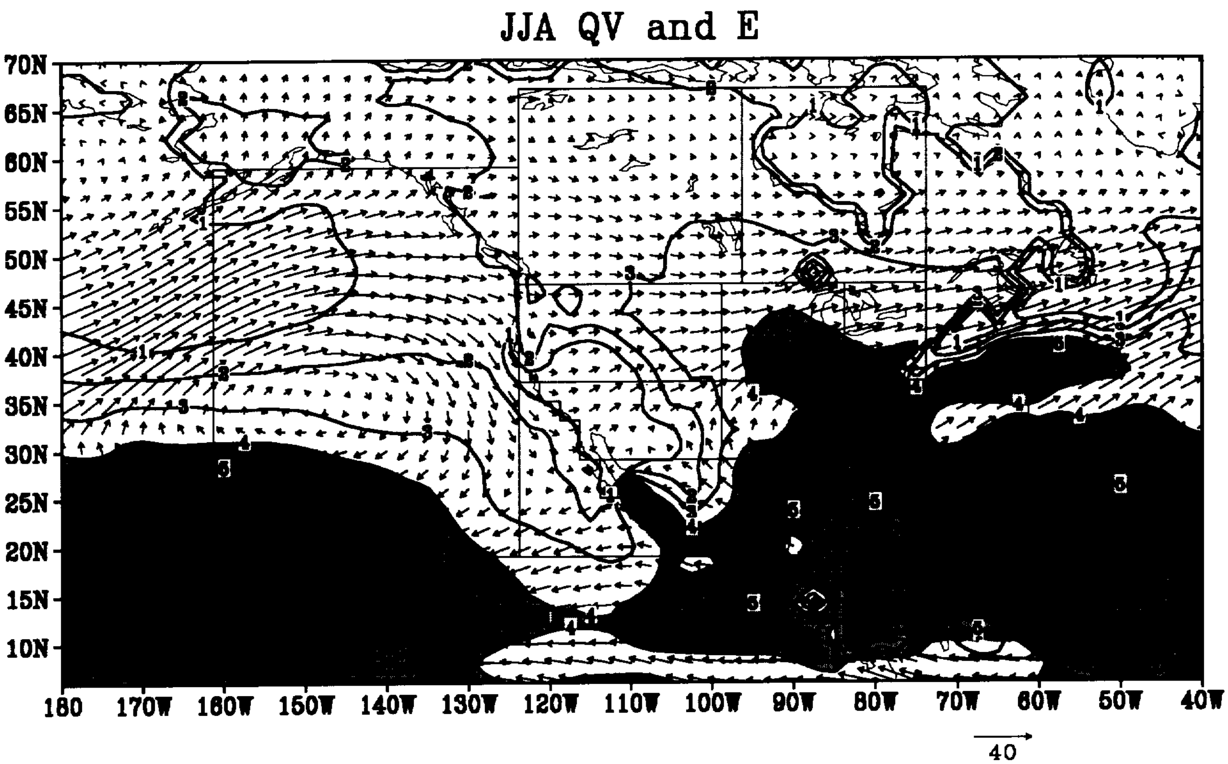
JJA QV and E
70N
65N
60N
55N
50N
45N
40N
35N
30N
25N
20N
15N
10N
180
170W
160W
150W
140W
130W
120W
110W
100W
90W
80W
70W
60W
50W
40W
40

Figure 8

Midwest US Water Sources

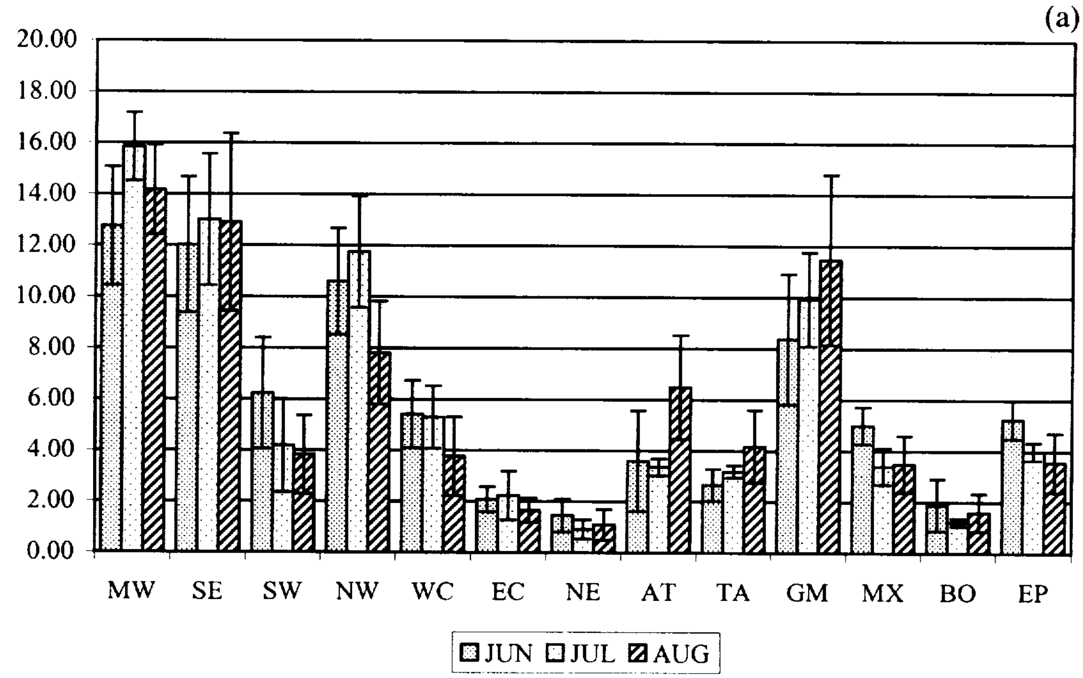

Southeast US Water Sources

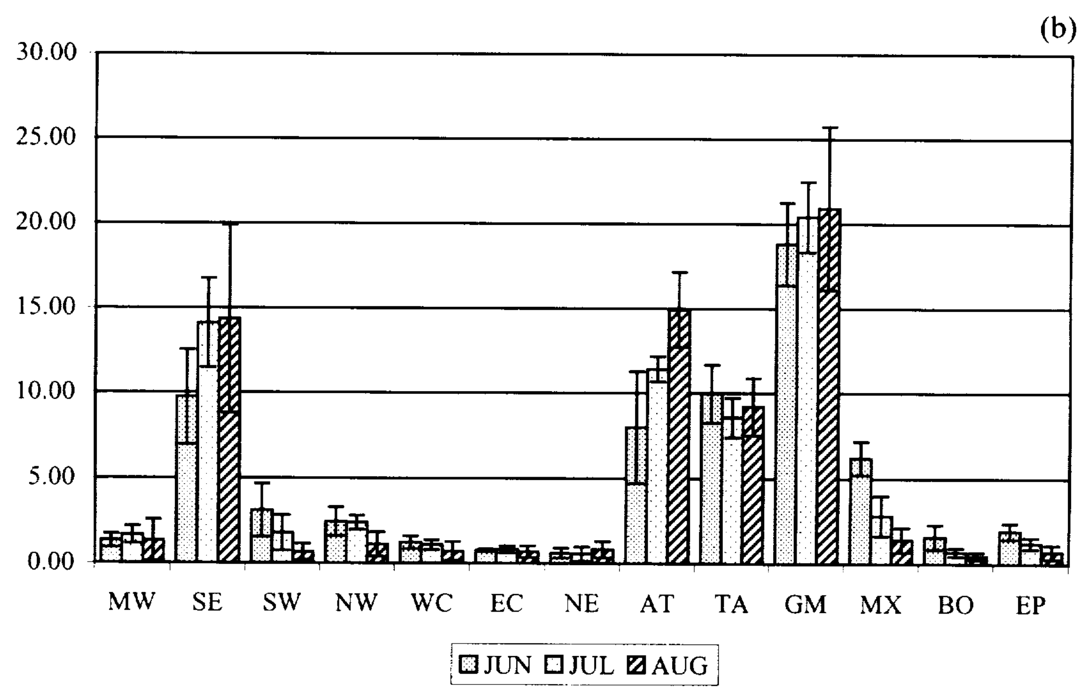

Figure 9

Southwest US Water Sources

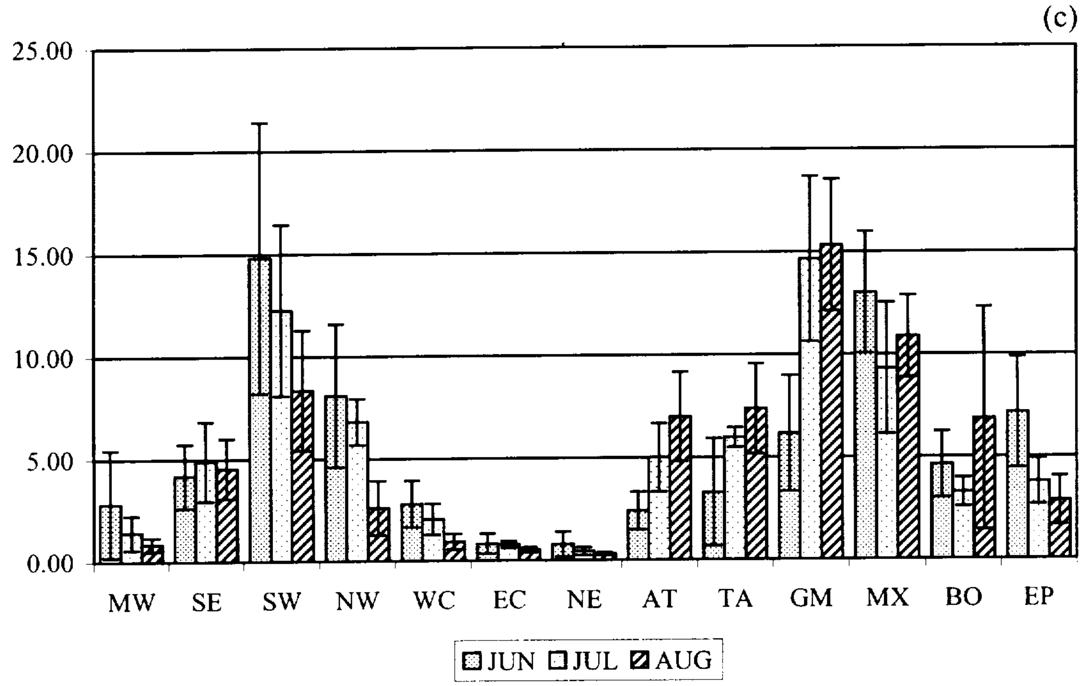

Mexico Water Sources

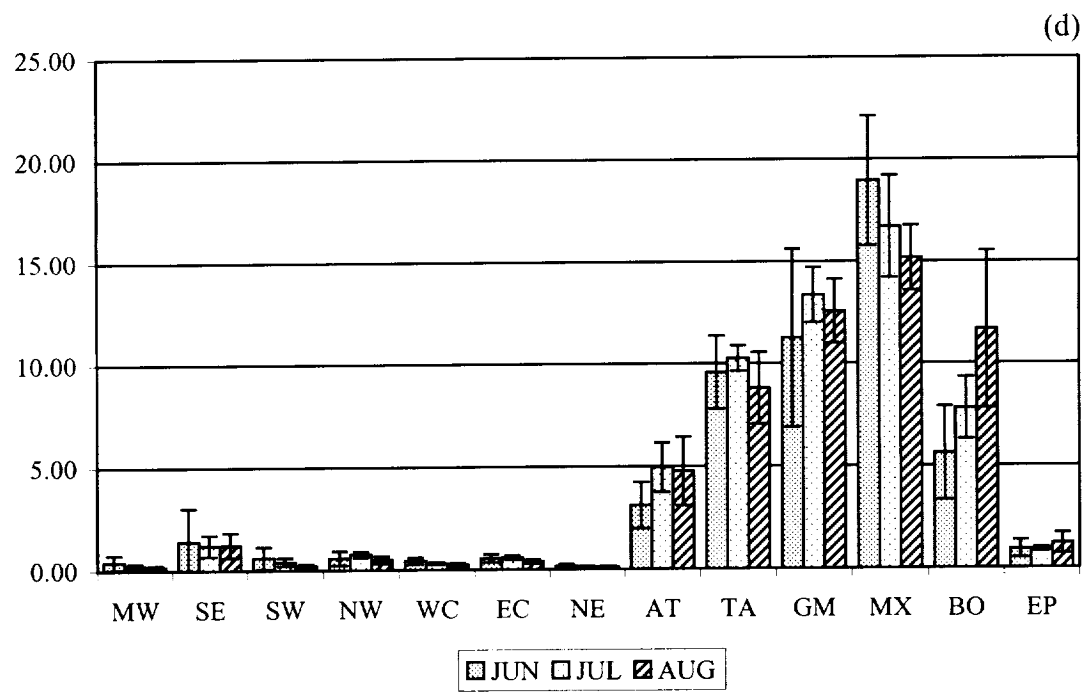

Figure 9

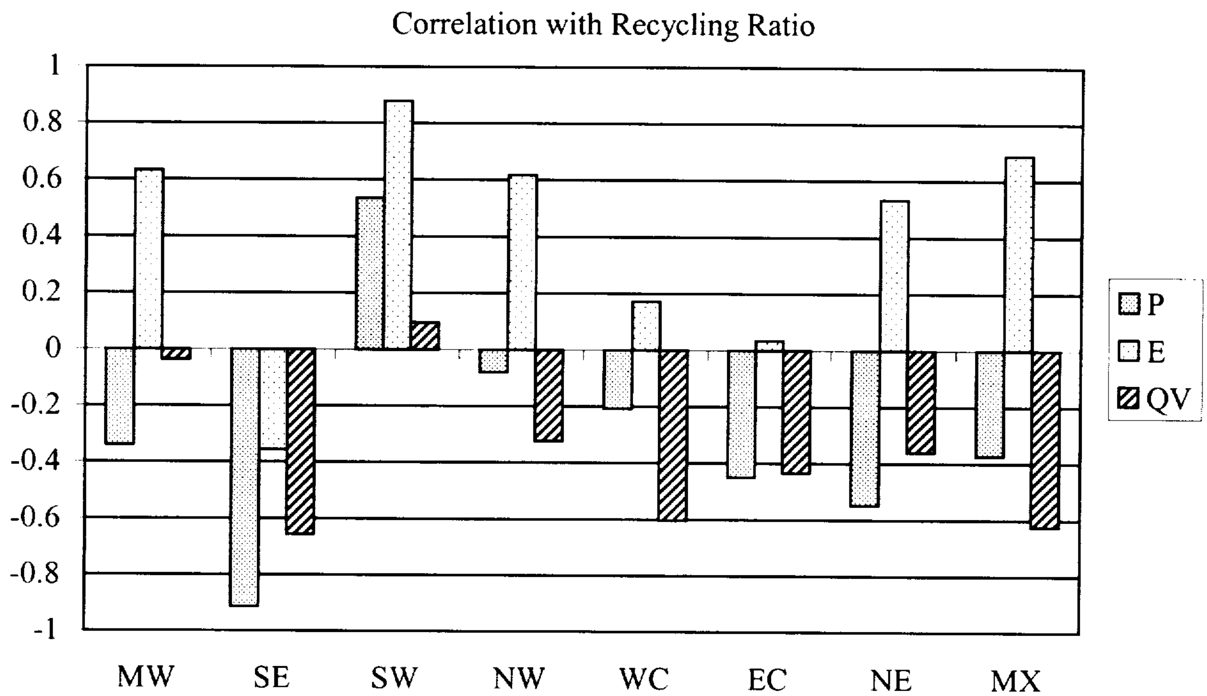
Correlation with Recycling Ratio
1
0.8
0.6
0.4
0.2
0
-0.2
-0.4
-0.6
-0.8
-1
MW
SE
SW
NW
WC
EC
NE
MX
P
E
QV

Figure 10

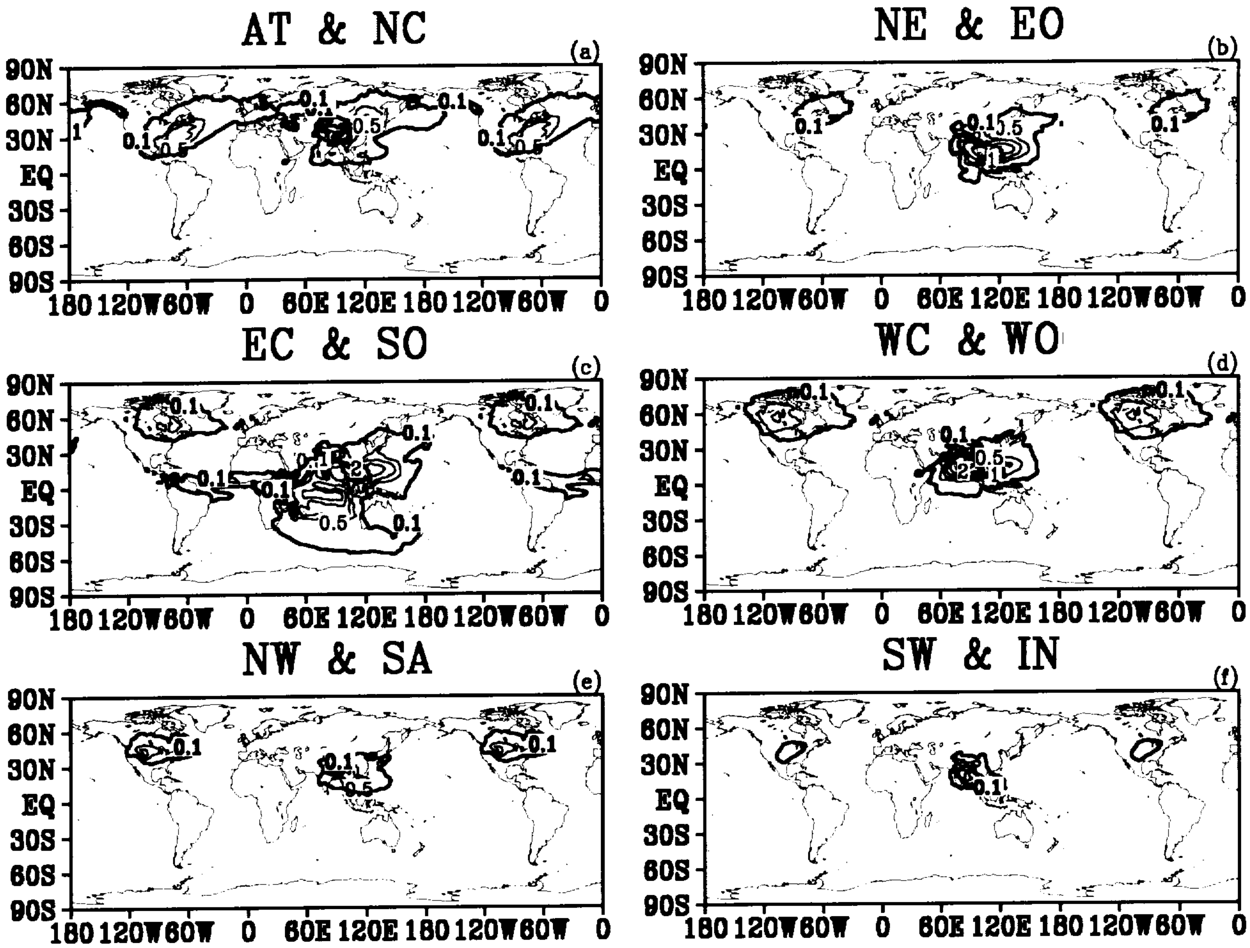
AT & NC
(a)
NE & EO
(b)
EC & SO
(c)
WC & WO
(d)
NW & SA
(e)
SW & IN
(f)
90N
60N
30N
EQ
30S
60S
90S
180 120W 60W 0 60E 120E 180 120W 60W 0

Figure 11

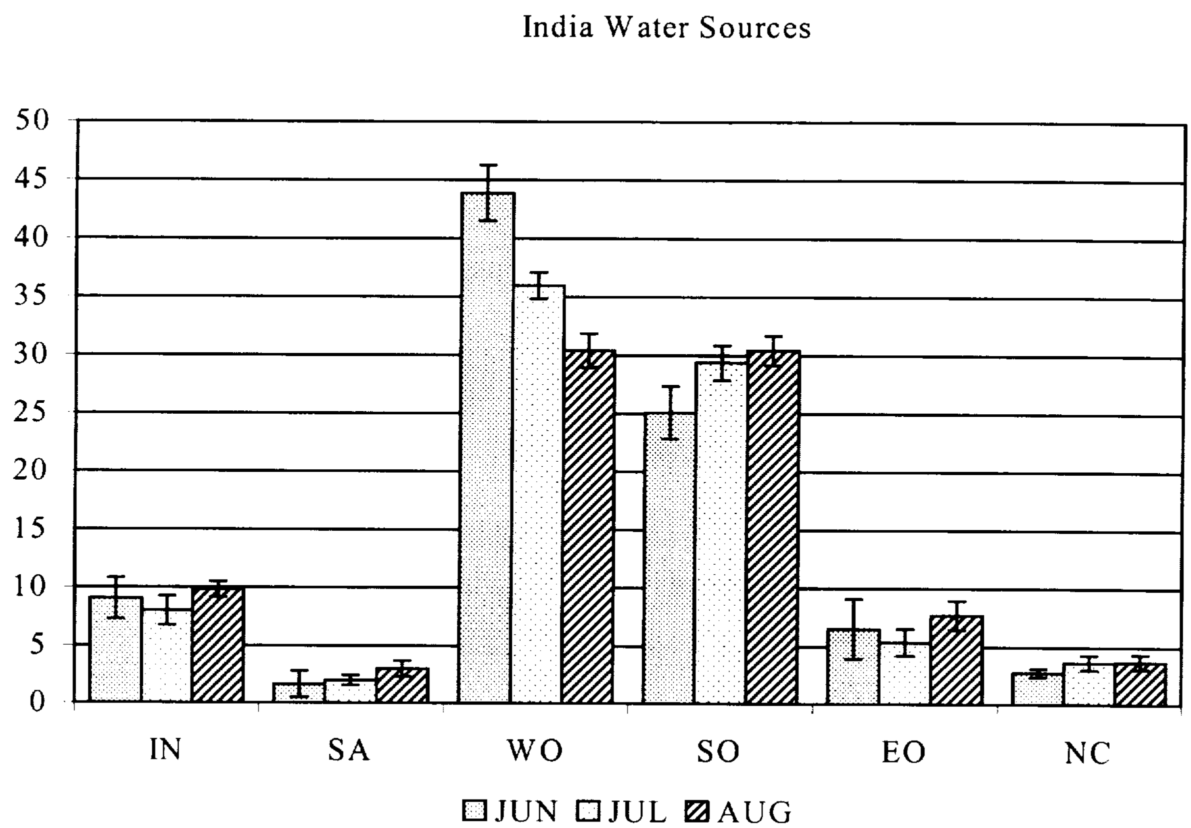
India Water Sources
50
45
40
35
30
25
20
15
10
5
0
IN
SA
WO
SO
EO
NC
JUN
JUL
AUG

Figure 12

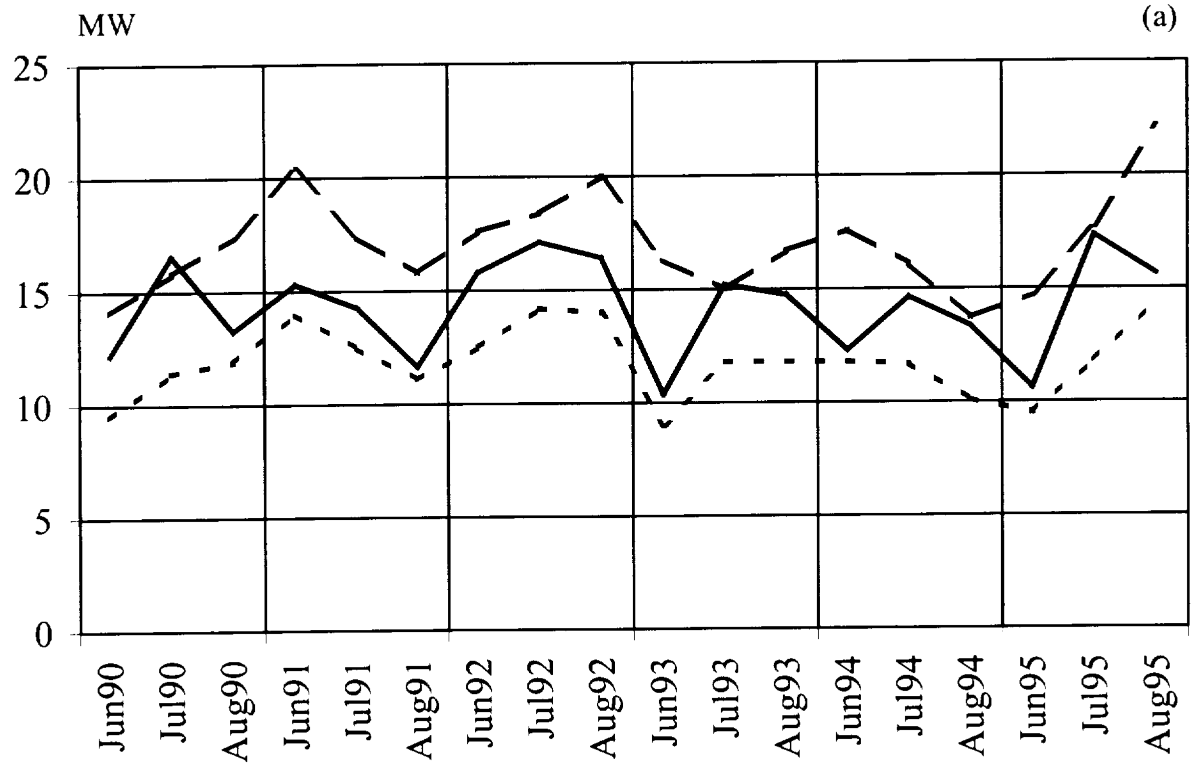
MW
(a)
25
20
15
10
5
0
Jun90
Jul90
Aug90
Jun91
Jul91
Aug91
Jun92
Jul92
Aug92
Jun93
Jul93
Aug93
Jun94
Jul94
Aug94
Jun95
Jul95
Aug95

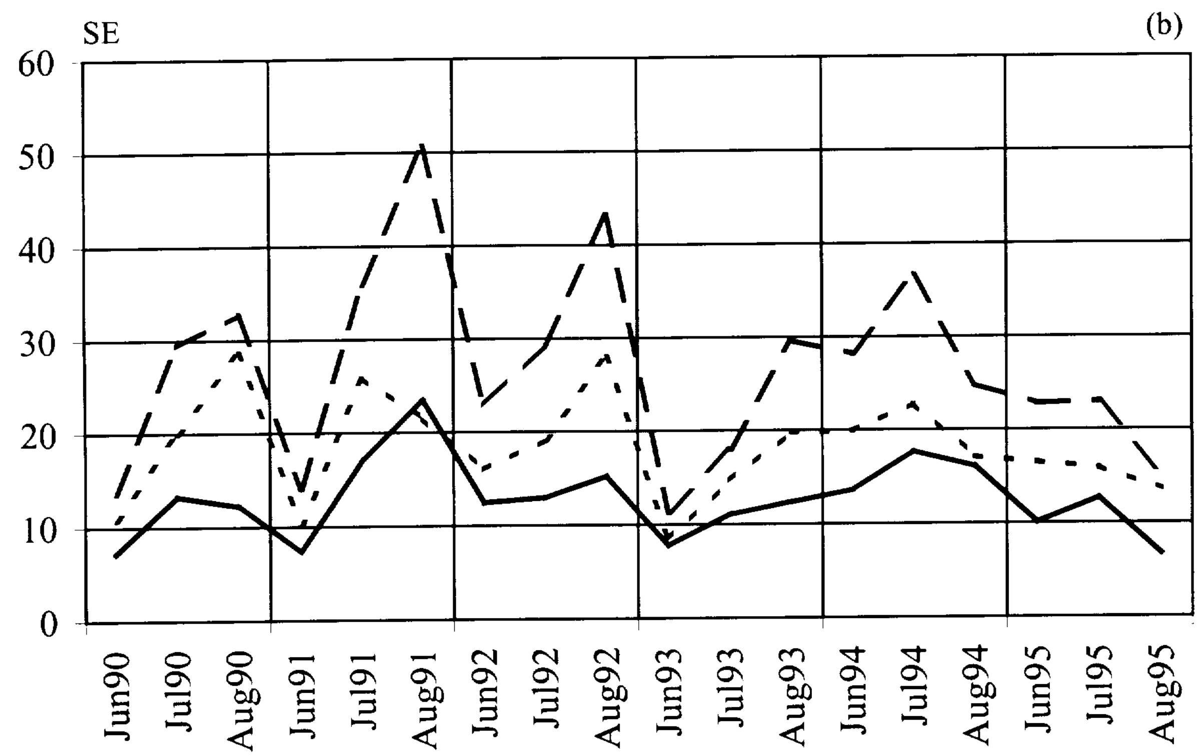
SE
(b)
60
50
40
30
20
10
0
Jun90
Jul90
Aug90
Jun91
Jul91
Aug91
Jun92
Jul92
Aug92
Jun93
Jul93
Aug93
Jun94
Jul94
Aug94
Jun95
Jul95
Aug95

Figure 13